Image-Current Mediated Sympathetic Laser Cooling of a Single Proton in a Penning Trap Down to 170 mK Axial Temperature

C. Will,[1] M. Wiesinger,[1] P. Micke,[1,2,*] H. Yildiz,[3] T. Driscoll,[1,4,†] S. Kommu,[3] F. Abbass,[3] B. P. Arndt,[1,5,6] B. B. Bauer,[3] S. Erlewein,[2,5] M. Fleck,[5,7] J. I. Jäger,[1,2,5] B. M. Latacz,[2,5] A. Mooser,[1] D. Schweitzer,[3] G. Umbrazunas,[5,8] E. Wursten,[5] K. Blaum,[1] J. A. Devlin,[9] C. Ospelkaus,[10,11] W. Quint,[6] A. Soter,[8] J. Walz,[3,12] C. Smorra,[3] and S. Ulmer[5,13]

(BASE Collaboration)

[1]*Max-Planck-Institut für Kernphysik, Saupfercheckweg 1, D-69117 Heidelberg, Germany*
[2]*CERN, 1211 Geneva, Switzerland*
[3]*Institut für Physik, Johannes Gutenberg-Universität, Staudingerweg 7, D-55128 Mainz, Germany*
[4]*Department of Physics, The University of Texas at Austin, Austin, Texas 78712, USA*
[5]*RIKEN, Fundamental Symmetries Laboratory, 2-1 Hirosawa, Wako, Saitama 351-0198, Japan*
[6]*GSI Helmholtzzentrum für Schwerionenforschung GmbH, D-64291 Darmstadt, Germany*
[7]*Graduate School of Arts and Sciences, University of Tokyo, Tokyo 153-8902, Japan*
[8]*Eidgenössische Technische Hochschule Zürich, John-von-Neumann-Weg 9, 8093 Zürich, Switzerland*
[9]*Centre for Cold Matter, Blackett Laboratory, Imperial College London, Prince Consort Road, London SW7 2AZ, United Kingdom*
[10]*Institut für Quantenoptik, Leibniz Universität Hannover, D-30167 Hannover, Germany*
[11]*Physikalisch-Technische Bundesanstalt, D-38116 Braunschweig, Germany*
[12]*Helmholtz-Institut Mainz, D-55099 Mainz, Germany*
[13]*Heinrich Heine University, Düsseldorf, Universitätsstrasse 1, D-40225 Düsseldorf, Germany*

(Received 9 October 2023; accepted 28 May 2024; published 12 July 2024)

We demonstrate a new temperature record for image-current mediated sympathetic cooling of a single proton in a cryogenic Penning trap by laser-cooled $^9Be^+$. An axial mode temperature of 170 mK is reached, which is a 15-fold improvement compared to the previous best value. Our cooling technique is applicable to any charged particle, so that the measurements presented here constitute a milestone toward the next generation of high-precision Penning-trap measurements with exotic particles.

DOI: 10.1103/PhysRevLett.133.023002

Laser cooling of atoms and ions is a widely employed method in the field of atomic physics [1,2]. However, only few species offer a suitable optical transition for laser cooling. For most other particles, sympathetic cooling techniques have to be employed. In the established sympathetic cooling schemes, the coupling is realized through direct ion-ion Coulomb interaction, where the charged particles are either trapped in the same potential well [3–5] or in two separate ones whose separation distance is a few hundred micrometers only [6,7].

Our group has recently demonstrated the sympathetic laser cooling of a single proton mediated by image currents [8]. Here, the two ion species are placed in two independent Penning traps that are separated by a distance of 5.5 cm but are connected to the same parallel resistor-inductor-capacitor (RLC) circuit [9]. This separation allows for cooling arbitrary trapped charged particles, including negatively charged particles such as antiprotons or the antihydrogen molecular ion $\bar{H}_2^-$, highly charged ions, molecular ions, and radioactive ions. Since many precision experiments with trapped ions are limited by particle temperature, a wide range of physics applications can be advanced with this cooling technique. These applications include *CPT*-reversal symmetry tests via magnetic moment and charge-to-mass ratio measurements with protons and antiprotons [10–12], magnetic moment measurements of light nuclei [13], tests of quantum electrodynamics via precision (mass) spectroscopy of highly charged ions [14,15], tests of the electroweak force with single molecular ions [16], as well precision mass measurements of radioactive ions [17]. Furthermore, in comparison to resistive cooling with a

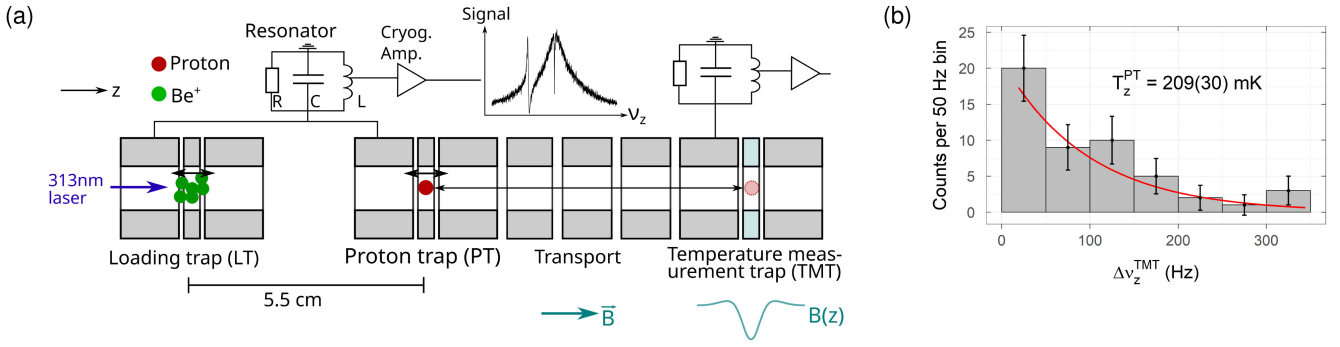

FIG. 1. (a) Schematic of the experimental setup. A cloud of beryllium ions is trapped in the loading trap (LT) and a single proton in the proton trap (PT). Both traps are connected to a common resonator. The proton is transported from the PT into the temperature measurement trap (TMT) for measuring its modified cyclotron energy via a quadratic magnetic field inhomogeneity. (b) Typical Boltzmann distribution of a temperature measurement. The red line corresponds to the Boltzmann distribution with a temperature as determined by the maximum-likelihood method.

cyclotron resonator [11,18], which is a standard cooling technique in high-precision Penning-trap experiments, the sympathetic cooling technique is widely tunable and applicable to all relevant q/m simultaneously instead of covering a single fixed particle charge-to-mass ratio q/m only. The lowest axial temperature achieved in Ref. [8] was (2.6 ± 2.5) K, measured via the temperature-induced axial frequency shift of only 100 mHz/K (axial) of the proton in the presence of an anharmonic trapping potential. This temperature measurement method requires that the beryllium ion cloud is laser cooled comparably strongly, which is detrimental to the achievable proton temperature as it reduces the effective image-current coupling strength [[19], Sec. 6.5.2].

In this Letter, we demonstrate axial temperatures of a single proton in a Penning trap down to about 170 mK, which constitutes a factor of 15 improvement compared to the previous record. To achieve this, a new temperature measurement trap (TMT) has been implemented that offers temperature resolution in the mK-range due to an axial frequency shift of 470 Hz/K (axial) arising from an optimized quadratic magnetic field inhomogeneity [[20], Sec. 4.1.3]. In addition, the cooling process has been optimized through numerical simulations [[19,21], Sec. 6.5]. Our sympathetic cooling experiments are performed in a cryogenic multi-Penning-trap system [[20], Sec. 4.1] [[19], Sec. 3.2.] that stores ions by means of a superposition of a homogeneous magnetic field of $B_0 \approx 1.9$ T and a quadrupolar electric potential, shown schematically in Fig. 1(a). The resulting harmonic motion of a single particle consists of the magnetron and modified cyclotron motion in the radial plane and an axial motion orthogonal to it with frequencies ν_-, ν_+, and ν_z, respectively [22]. The axial motion of a particle is detected by tuning its axial frequency to the resonance frequency ν_0 of a parallel RLC circuit (also called resonator) with high effective parallel resistance R and thus high quality factor Q, which is excited by thermal Johnson-Nyquist noise [23]. In our case, $\nu_0^{\mathrm{PTLT}} = 345\,250$ Hz and $Q \approx 10\,000$ for the resonator that is connected to both the proton trap (PT) and loading trap (LT) [[20], Sec. 4.1.4]. The voltage signal of the resonator is amplified by a cryogenic low-noise amplifier at 4 K [24] followed by another amplification stage at room temperature. The fast Fourier transform of the resonator voltage signal yields the characteristic spectrum featuring a dip at the ion's axial frequency [23], shown schematically in the inset of Fig. 1(a). The coupling of the particles to the resonator is given by their respective dip width $\gamma_z = (1/2\pi)(R/m)(q^2/D^2)N$, where N is the number of ions of the species and D an effective trap size [23]. The cooling measurements are performed with a single proton in the PT and a cloud of beryllium ions in the LT with dip widths of 2.2 Hz and 0.10 Hz per ion, respectively. The common resonator mediates the energy exchange via image currents between the particles [8]. The proton is sympathetically cooled by tuning the axial frequency of both species to the resonator frequency and laser cooling the beryllium ions via the 313 nm $^2S_{1/2} \rightarrow {}^2P_{3/2}$ transition with a natural linewidth of $\Gamma \approx 2\pi \times 20$ MHz [25].

To measure the temperature of the proton, we employ a two-trap measurement scheme. Since the resonator constitutes a thermal reservoir, the axial mode continuously samples a Boltzmann distribution with a correlation time of $1/\gamma_z$ if $\nu_z \approx \nu_0$. The corresponding time average is, according to the ergodic theorem, equivalent to the ensemble average which we use as the temperature definition of a single particle. In contrast, the modified cyclotron mode remains at constant energy. However, it can be coupled to the axial mode by irradiating a quadrupolar sideband drive at frequency $\nu_{\mathrm{rf}} = \nu_+ - \nu_z$ [26]. In this way, an axial energy is imprinted on the modified cyclotron mode. The corresponding temperatures obey the relation $T_+ = (\nu_+/\nu_z)T_z$, where T_+ and T_z are the temperatures of the modified cyclotron mode and the axial mode, respectively. After turning off the drive, the modified cyclotron energy E_+ of the proton stays constant and the

proton is transported from the PT into the TMT, where E_+ is measured. The TMT features a ferromagnetic ring electrode, which introduces a large quadratic magnetic field inhomogeneity, i.e., $B_z^{\mathrm{TMT}}(z) = B_0^{\mathrm{TMT}} + B_2^{\mathrm{TMT}} z^2$, with $B_2^{\mathrm{TMT}} = 27.8(7)\ \mathrm{kT/m^2}$ [[20], Sec. 4.1.3] [[19], Sec. 7.2.3]. To measure E_+, we utilize the fact that the B_2 coefficient causes an axial frequency shift in the TMT that is proportional to E_+ [22,27]; in our case $\delta\nu_z^{\mathrm{TMT}}/\delta E_+ = 5.8\ \mathrm{Hz}/(\mathrm{K} \times k_B)$ for the proton. Thus, by recording the proton's axial frequency in the TMT compared to the unshifted one, its momentary E_+ is measured. Finally, the proton is transported back to the PT. This protocol is repeated and the resulting distribution of E_+ is used to derive the temperature. An example of such a Boltzmann distribution is given in Fig. 1(b).

In order to convert the distribution of axial frequency measurements in the TMT to an axial temperature in the PT, T_z^{PT}, we calculate its maximum-likelihood estimator, given by

$$T_z^{\mathrm{PT}} = \frac{\nu_z^{\mathrm{PT}}}{\nu_+^{\mathrm{PT}}} \frac{B_0^{\mathrm{PT}}}{B_2^{\mathrm{TMT}}} \frac{4\pi^2}{k_{\mathrm{B}}} m \nu_{z,0}^{\mathrm{TMT}} \langle \nu_z^{\mathrm{i,TMT}} - \nu_{z,0}^{\mathrm{TMT}} \rangle. \quad (1)$$

Here, $\nu_{z,0}^{\mathrm{TMT}} \approx 550\,875$ Hz is the unshifted axial frequency in the TMT at $E_+ = 0$ and $\nu_z^{\mathrm{i,TMT}}$ are the individual axial frequency measurements. $B_0^{\mathrm{PT}} = 1.899$ T is the magnetic field in the PT and $\nu_+^{\mathrm{PT}} \approx 28.9$ MHz and $\nu_z^{\mathrm{PT}} = 345\,250$ Hz are the modified cyclotron and axial frequencies of the proton in the PT, respectively, and k_{B} is Boltzmann's constant. This formula incorporates not only the axial frequency shift due to nonzero E_+, but also the temperature relation due to sideband coupling and the relative modified cyclotron energy change during transport into a different magnetic field, in our case by the magnetic field ratio of the traps, $B_0^{\mathrm{PT}}/B_0^{\mathrm{TMT}}$.

In support of the experimental effort, we performed first-principles simulations of the experimental setting that is shown in Fig. 1(a) [21] [[19], Sec. 6]. We found that the cooling scheme can be understood by the formation of a symmetric and antisymmetric normal mode of the axial motion of the coupled proton-beryllium system. The antisymmetric mode decouples partially from the resonator due to image-current cancellation, so that the laser cools it close to the Doppler limit. In contrast, the symmetric mode couples and thermalizes to the resonator and the relative proton and $^9\mathrm{Be}^+$ component are given by their respective dip widths. Since image-current coupling relies on the motion of the particles, for a minimal proton temperature the damping rate of the cooling laser γ_{L} must be sufficiently weak in order to not decouple the beryllium ions from the resonator, i.e., $\gamma_{\mathrm{L}} \ll \gamma_{z,\mathrm{Be}}$, where $\gamma_{z,\mathrm{Be}}$ denotes the dip width of the beryllium cloud. Then, the axial temperature of a proton with dip width $\gamma_{z,\mathrm{p}}$ is given by [21] [[19], Sec. 6.5.2]

$$T_{z,\mathrm{p}} = \frac{1}{1 + \frac{\gamma_{z,\mathrm{Be}}}{\gamma_{z,\mathrm{p}}}} T_{\mathrm{res}}, \quad (2)$$

where T_{res} is the effective noise temperature of the resonator. In order to compare theory with experiment, T_{res} is measured as the first preparatory step to $T_{\mathrm{res}} = (8.6 \pm 0.8)$ K using the TMT and a single proton with no beryllium ions loaded. The cryogenic amplifier is turned off for this measurement as well as for the sympathetic cooling measurements, since otherwise the amplifier's input noise gives rise to a slightly higher effective axial temperature.

For efficient sympathetic cooling, it is crucial to minimize the axial frequency difference of the two species to below the sympathetic cooling rate such that stable symmetric and antisymmetric modes are preserved. Hence, in the following their individual frequency stabilities are examined. The axial frequency stability of the single proton in the PT is $\sigma(\nu_{z,\mathrm{p}}) \approx 40$ mHz for 60 s averaging time, which is sufficiently small. In contrast, the axial frequency stability of the beryllium ion cloud is adversely affected by the radial cloud expansion due to the Coulomb interaction [28,29]. In order to prevent an uncontrolled radial expansion, the radial modes of a large beryllium cloud must be regularly cooled. However, in our setup the laser is applied nearly parallel to the trap axis so that the cooling of radial modes [30] is not efficient. Since large laser powers are not feasible because the cooling scheme requires low photon scattering rates, a magnetron sideband drive at $\nu_{\mathrm{rf}} = \nu_{z,\mathrm{Be}} + \nu_{-,\mathrm{Be}}$ [26] is applied in addition to the cooling laser. We observe axial frequency drifts of the beryllium ion clouds after turning off the magnetron sideband drive, as shown exemplarily in Fig. 2 for two ion clouds of 840 ions and 2000 ions [[20], Sec. 4.7] [[19], Sec. 9.1]. These drifts are related to the harmonicity of the electrical trap potential, which is adjustable via the tuning ratio (TR) of the trap as defined in Ref. [22]. We attribute these frequency drifts to the change in the aspect ratio of the beryllium ion cloud while the cloud expands due to Coulomb repulsion in an anharmonic trapping potential [29]. The accumulated frequency shift can be reset by applying the magnetron sideband drive again. Figure 2(a) demonstrates that a TR optimization allows to control the frequency drifts of clouds of $\lesssim$1000 ions to < 1 Hz on the relevant timescale, which is sufficiently stable for the sympathetic cooling process. In contrast, for larger clouds the drifts are not only stronger, they also exhibit a quadratic component, as shown in Fig. 2(b). For large clouds above 1000 ions, this requires us to introduce small frequency offsets and apply the cooling procedure during the times when the change in ion-ion frequency detuning is minimal.

With the TR adjusted on a permille level, we were able to sufficiently stabilize beryllium ion clouds with dip widths of up to 120 Hz or 1200 ions. Assuming the proton is initially trapped in the PT, one sympathetic cooling cycle consists of the following steps [[19], Sec. 9.3]: First, in

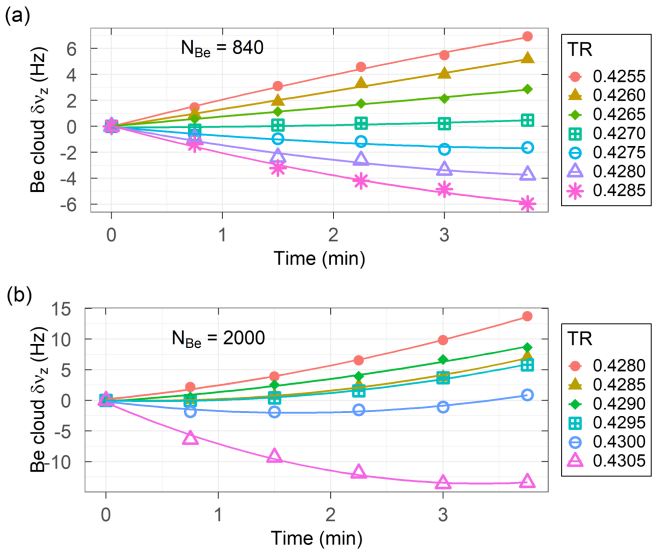

FIG. 2. Axial frequency drift of a cloud of beryllium ions in the LT after applying the magnetron sideband drive at $\nu_{\mathrm{rf}} = \nu_{\mathrm{z,Be}} + \nu_{-,\mathrm{Be}}$. The drift is related to the tuning ratio (TR) of the trap [20] and becomes stronger the larger the cloud is.

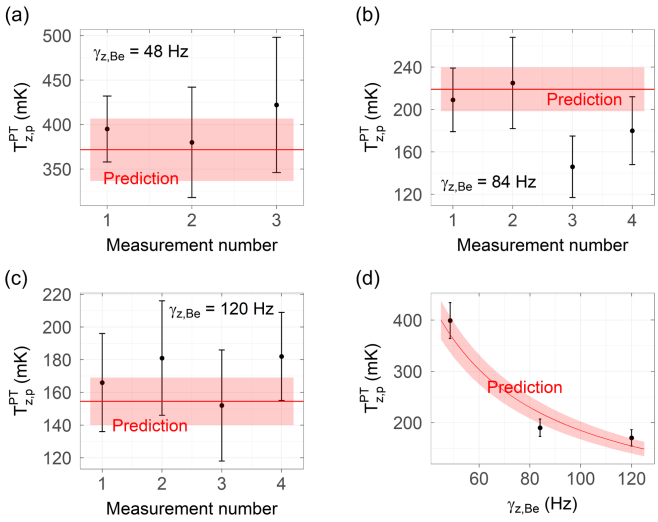

FIG. 3. Axial temperature measurements of a sympathetically cooled proton. Three differently sized beryllium ion clouds were employed. The red line is the prediction by Eq. (2) and the shaded red area the associated uncertainty. In (d) the individual measurements for each cloud size are combined and plotted as a function of the beryllium ion cloud dip width $\gamma_{\mathrm{z,Be}}$, which is proportional to the number of trapped $^9\mathrm{Be}^+$.

order to start the cooling process, the axial frequencies of the proton and beryllium ion cloud are matched in between two iterations of applying the magnetron sideband drive to the beryllium ion cloud. The cooling laser is kept continuously on with a weak damping rate during the whole cycle. During the sympathetic cooling, the modified cyclotron sideband frequency of the proton is continuously applied at $\nu_{\mathrm{rf}} = \nu_{+,\mathrm{p}} - \nu_{\mathrm{z,p}}$ with about 1 Hz Rabi frequency. The total cooling time is set to 90 s. The cooling time constant has not been explicitly measured, however, it was verified that after 90 s the resulting temperatures have converged and two subsequent values of E_+ are uncorrelated. Afterwards, the proton is transported into the TMT to measure E_+. Finally, the proton is transported back into the PT and the next cooling cycle is carried out. A single temperature measurement consists of > 20 individual cooling cycles.

This cooling process has been conducted for three differently sized beryllium ion clouds with dip widths of 48, 84, and 120 Hz, corresponding to 480, 840, and 1200 ions. For the 48 Hz cloud, the cooling laser was set to 84 MHz red detuning and its power was adjusted to 5–15 μW, which corresponds to 1.5%–4.5% of the saturation power of the cooling transition. The saturation power of $P_{\mathrm{sat}} = 340$ μW was measured by in-trap detection of fluorescence photons [20,31]. For the 84 and 120 Hz clouds, the laser power and red detuning were increased to 100 μW and 200 MHz, respectively, motivated by a vanishing of unidentified heating effects of the beryllium ion cloud. In contrast to our previous work [8], both parameter sets fulfill the condition that the beryllium ion cloud is damped only weakly and that no loss of the SNR of the beryllium dip occurs. Several independent proton temperature measurements have been conducted for each beryllium cloud with results shown in Fig. 3, where the uncertainty of each temperature measurement is dominated by the statistical uncertainty. The horizontal red line is the temperature predicted by Eq. (2) and the shaded red area is the corresponding uncertainty, which is dominated by the statistical uncertainty of the measurement of T_{res}. In general, we observe excellent agreement between the theoretical prediction and the experimental data. The lowest reproducibly measured temperature of about 170 mK constitutes a 15-fold improvement compared to the previous record measurement [8]. We emphasize that not only the temperatures agree, but also the method to reach them. The prediction by the simulations that a weak laser damping rate is required [21] has been confirmed as well.

Moreover, our results demonstrate the capability of the two-trap temperature measurement technique. By separating the temperature determination from the cooling process a broad range of temperatures between 5 mK and 10 K can be measured and resolved. In this regard we also measured a negligible heating rate of $\lesssim 2$ mK (axial-equivalent) per cycle, which incorporates all heating rates of the cyclotron mode the proton might be subject to. For this measurement, we repeated the cooling sequence but detuned the modified cyclotron sideband frequency for the proton by 10 kHz [[19], Sec. 7.4.2].

Further, we study the effect of a relative axial frequency detuning between the proton and the beryllium ion cloud, since the resulting width can be considered a measure of the sympathetic cooling rate and provides a reference for the

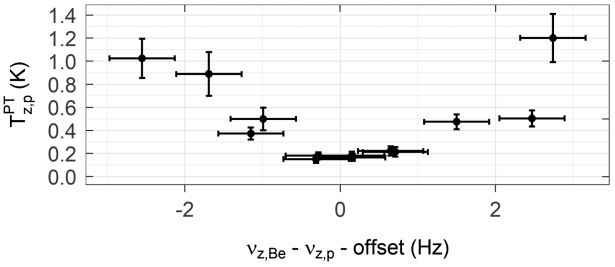

FIG. 4. Temperature of the sympathetically cooled proton as a function of relative axial frequency detuning between the proton and beryllium ions. The data was recorded with 1200 $^9Be^+$.

required particle frequency stabilities. To this end, the 120 Hz cloud was tuned to slightly different axial frequencies than the proton. All other steps remain the same as before. The resulting proton temperatures are shown in Fig. 4. Notably, these measurements were also recorded with the cryogenic amplifier turned off, so that the relative frequency detuning is estimated based on the initial center frequency as well as the TR-related frequency drift. This gives rise to a small offset of about 2 Hz. Nevertheless, the existence of a cooling resonance is evident and the minimum corresponds within uncertainty to the prediction by Eq. (2).

In summary, we have demonstrated image-current mediated sympathetic cooling of a single proton to axial temperatures of 170 mK, which is a factor of 50 below the environment temperature and a 15-fold improvement compared to the previous record [8]. As such, this work constitutes a crucial milestone toward the next generation of high-precision Penning-trap measurements with particles that require sympathetic cooling with separate trapping regions.

Several routes toward lower proton temperatures are conceivable. An optimized beryllium ion trap for which the dip width per beryllium ion is maximized and the anharmonicity-related frequency drifts are minimized would directly enable lower proton temperatures. Alternatively, with an independent cooling laser in radial direction it would be possible to control significantly larger beryllium ion clouds via laser cooling only. Then, the magnetron sideband coupling with its associated frequency drifts would become obsolete. Another option would be to confine larger beryllium ion clouds radially with a rotating wall potential [32]. Besides, the simulation studies [21] as well as independent work in Ref. [33] predict that a cooling scheme with several kHz particle-resonator detuning and pulsed laser cooling can achieve 10 mK axial particle temperatures with about 100 beryllium ions only. Although these advanced cooling methods require significant additional experimental effort such as the operation of a cryogenic frequency switch [[20], Sec. 5.8.3] or the control of $>10^4$ beryllium ions to sub-Hz axial frequency stability, the excellent agreement between experiment and simulation in this work further corroborates their fundamental feasibility.

The fact that all these cooling schemes rely on image-current coupling makes them in principle applicable to any trapped charged particle and experimental systems beyond Penning traps [34]. In particular, once even lower temperatures of about 10 mK (axial) can be reached [35], the sympathetic cooling will significantly boost the sampling rate and spin state detection fidelity [36,37] of future g-factor measurements on protons [10], antiprotons [11], and other nuclear moments, as well as reduce the dominant systematic uncertainties in mass measurements with the highest precision [12].

We acknowledge financial support from the Max-Planck-Society, the RIKEN Chief Scientist Program, the RIKEN Pioneering Project Funding, the RIKEN JRA Program, the Helmholtz-Gemeinschaft, the DFG through SFB 1227 "DQ-mat," the cluster of excellence QuantumFrontiers, the CERN Gentner programme, the Max-Planck IMPRS-PTFS, the European Research Council (ERC) under the European Union's Horizon 2020 research and innovation programme (Grant agreements No. 832848—FunI, No. 721559—AVA, No. 852818—STEP), and the Max-Planck–RIKEN–PTB Center for Time, Constants, and Fundamental Symmetries.

*Present address: Helmholtz Institute Jena, GSI Helmholtz Centre for Heavy Ion Research, Planckstraße 1, 64291 Darmstadt, Germany.

†Present address: The University of Oregon, Eugene, Oregon 97403, USA.

[1] C. N. Cohen-Tannoudji, Rev. Mod. Phys. **70**, 707 (1998).

[2] M. S. Safronova, D. Budker, D. DeMille, D. F. J. Kimball, A. Derevianko, and C. W. Clark, Rev. Mod. Phys. **90**, 025008 (2018).

[3] D. J. Larson, J. C. Bergquist, J. J. Bollinger, W. M. Itano, and D. J. Wineland, Phys. Rev. Lett. **57**, 70 (1986).

[4] S. M. Brewer, J.-S. Chen, A. M. Hankin, E. R. Clements, C. W. Chou, D. J. Wineland, D. B. Hume, and D. R. Leibrandt, Phys. Rev. Lett. **123**, 033201 (2019).

[5] P. Micke, T. Leopold, S. A. King, E. Benkler, L. J. Spieß, L. Schmöger, M. Schwarz, J. R. Crespo López-Urrutia, and P. O. Schmidt, Nature (London) **578**, 60 (2020).

[6] M. Harlander, R. Lechner, M. Brownnutt, R. Blatt, and W. Hänsel, Nature (London) **471**, 200 (2011).

[7] K. R. Brown, C. Ospelkaus, Y. Colombe, A. C. Wilson, D. Leibfried, and D. J. Wineland, Nature (London) **471**, 196 (2011).

[8] M. Bohman, V. Grunhofer, C. Smorra, M. Wiesinger, C. Will, M. J. Borchert, J. A. Devlin, S. Erlewein, M. Fleck, S. Gavranovic, J. Harrington, B. Latacz, A. Mooser, D. Popper, E. Wursten, K. Blaum, Y. Matsuda, C. Ospelkaus, W. Quint, J. Walz, and S. Ulmer, Nature (London) **596**, 514 (2021).

[9] D. J. Heinzen and D. J. Wineland, Phys. Rev. A **42**, 2977 (1990).
[10] G. Schneider, A. Mooser, M. Bohman, N. Schön, J. Harrington, T. Higuchi, H. Nagahama, S. Sellner, C. Smorra, K. Blaum, Y. Matsuda, W. Quint, J. Walz, and S. Ulmer, Science **358**, 1081 (2017).
[11] C. Smorra, S. Sellner, M. J. Borchert, J. A. Harrington, T. Higuchi, H. Nagahama, T. Tanaka, A. Mooser, G. Schneider, M. Bohman, K. Blaum, Y. Matsuda, C. Ospelkaus, W. Quint, J. Walz, Y. Yamazaki, and S. Ulmer, Nature (London) **550**, 371 (2017).
[12] M. J. Borchert *et al.*, Nature (London) **601**, 53 (2022).
[13] A. Mooser, A. Rischka, A. Schneider, K. Blaum, S. Ulmer, and J. Walz, J. Phys. Conf. Ser. **1138**, 012004 (2018).
[14] A. Egl, I. Arapoglou, M. Höcker, K. König, T. Ratajczyk, T. Sailer, B. Tu, A. Weigel, K. Blaum, W. Nörtershäuser, and S. Sturm, Phys. Rev. Lett. **123**, 123001 (2019).
[15] F. Heiße, M. Door, T. Sailer, P. Filianin, J. Herkenhoff, C. M. König, K. Kromer, D. Lange, J. Morgner, A. Rischka, C. Schweiger, B. Tu, Y. N. Novikov, S. Eliseev, S. Sturm, and K. Blaum, Phys. Rev. Lett. **131**, 253002 (2023).
[16] J. Karthein, S.-M. Udrescu, S. B. Moroch, I. Belosevic, K. Blaum, A. Borschevsky, Y. Chamorro, D. DeMille, J. Dilling, R. F. G. Ruiz, N. R. Hutzler, L. F. Pašteka, and R. Ringle, arXiv:2310.11192.
[17] V. V. Simon, U. Chowdhury, P. Delheij, J. Dilling, B. Eberhardt, and G. Gwinner, J. Phys. Conf. Ser. **312**, 052024 (2011).
[18] S. Ulmer, K. Blaum, H. Kracke, A. Mooser, W. Quint, C. Rodegheri, and J. Walz, Nucl. Instrum. Methods Phys. Res., Sect. A **705**, 55 (2013).
[19] C. Will, Sympathetic cooling of trapped ions coupled via image currents: Simulation and measurement, Ph.D. thesis, Ruperto-Carola University of Heidelberg, 2023, 10.11588/heidok.00033185.
[20] M. Wiesinger, Sympathetic cooling of a single individually-trapped proton in a cryogenic penning trap, Ph.D. thesis, Ruperto-Carola University of Heidelberg, 2023, 10.11588/heidok.00033334.
[21] C. Will, M. Bohman, T. Driscoll, M. Wiesinger, F. Abbass, M. J. Borchert, J. A. Devlin, S. Erlewein, M. Fleck, B. Latacz *et al.*, New J. Phys. **24**, 033021 (2022).
[22] L. S. Brown and G. Gabrielse, Rev. Mod. Phys. **58**, 233 (1986).
[23] D. J. Wineland and H. G. Dehmelt, J. Appl. Phys. **46**, 919 (1975).
[24] H. Nagahama, G. Schneider, A. Mooser, C. Smorra, S. Sellner, J. Harrington, T. Higuchi, M. Borchert, T. Tanaka, M. Besirli, K. Blaum, Y. Matsuda, C. Ospelkaus, W. Quint, J. Walz, Y. Yamazaki, and S. Ulmer, Rev. Sci. Instrum. **87**, 113305 (2016).
[25] T. Andersen, K. A. Jessen, and G. Sørensen, Phys. Rev. **188**, 76 (1969).
[26] E. A. Cornell, R. M. Weisskoff, K. R. Boyce, and D. E. Pritchard, Phys. Rev. A **41**, 312 (1990).
[27] J. Ketter, T. Eronen, M. Höcker, S. Streubel, and K. Blaum, Int. J. Mass Spectrom. **358**, 1 (2014).
[28] J. J. Bollinger, D. J. Heinzen, F. L. Moore, W. M. Itano, D. J. Wineland, and D. H. E. Dubin, Phys. Rev. A **48**, 525 (1993).
[29] C. S. Weimer, J. J. Bollinger, F. L. Moore, and D. J. Wineland, Phys. Rev. A **49**, 3842 (1994).
[30] W. M. Itano and D. J. Wineland, Phys. Rev. A **25**, 35 (1982).
[31] M. Wiesinger *et al.*, Rev. Sci. Instrum. **94**, 123202 (2023).
[32] S. Bharadia, M. Vogel, D. M. Segal, and R. C. Thompson, Appl. Phys. B **107**, 1105 (2012).
[33] B. Tu, F. Hahne, I. Arapoglou, A. Egl, F. Heiße, M. Höcker, C. König, J. Morgner, T. Sailer, A. Weigel, R. Wolf, and S. Sturm, Adv. Quantum Technol. **4**, 2100029 (2021).
[34] D. An, A. M. Alonso, C. Matthiesen, and H. Häffner, Phys. Rev. Lett. **128**, 063201 (2022).
[35] J. M. Cornejo, J. Brombacher, J. A. Coenders, M. von Boehn, T. Meiners, M. Niemann, S. Ulmer, and C. Ospelkaus, Phys. Rev. Res. **5**, 033226 (2023).
[36] C. Smorra, A. Mooser, M. Besirli, M. Bohman, M. Borchert, J. Harrington, T. Higuchi, H. Nagahama, G. Schneider, S. Sellner, T. Tanaka, K. Blaum, Y. Matsuda, C. Ospelkaus, W. Quint, J. Walz, Y. Yamazaki, and S. Ulmer, Phys. Lett. B **769**, 1 (2017).
[37] M. Bohman, A. Mooser, G. Schneider, N. Schön, M. Wiesinger, J. Harrington, T. Higuchi, H. Nagahama, C. Smorra, S. Sellner, K. Blaum, Y. Matsuda, W. Quint, J. Walz, and S. Ulmer, J. Mod. Opt. **65**, 568 (2018).